International Journal of Electrical Engineering and Sustainability (IJEES)
ISSN (online): 2959-9229
https://ijees.org/index.php/ijees/index
Arab Impact Factor: 1.51 Dolj 2026 = Q1
Volume 4 | Number 2 | July-December 2026 | Pages 171-192

Efficient and Reliable Dynamic Economic Dispatch for a Hybrid Power System

Abdullah K. Alazem[1*], Hamad A. Mohamed[2], Ali M. Yousef[3], Mahmoud I. Mohamed[4], Ahmed A. Hafez[5], Yasser F.Nassar[6], Hala J. El-Khozondar[7]

[1]Operating Department, Distribution Networks, Emergency Administration, Ministry of Electricity, Water & Renewable Energies, Kuwait
[2,3,4,5]Electrical Engineering Department, Assiut University, Assiut, Egypt
[6]Department of Mechanical and Renewable Energy Engineering, Faculty of Engineering, Wadi Alshatti University, Libya
[7]Department of Electrical Engineering and Smart Systems, Islamic University of Gaza, Palestine

Email: [1]akalazmi@mew.gov.kw, [2]hamad_az@aun.edu.eg, [3]Ali_affy@aun.edu.eg, [4]mahmoudmosaad@aun.edu.eg, , [5]prof.hafez@aun.edu.eg, [6]y.nassar@wau.edu.ly, [7]hkhozondar@iugaza.edu.ps

Received: June 06, 2026 Accepted: September 03, 2026 Published: September 14, 2026
DOI: 10.65998/ijees.v4i2.187

Abstract: Hybrid electrical power systems are recently the trend for securing sustainable and environmental compatibility electrical energy source. The article proposes Dynamic Economic Dispatch (DED) for running the hybrid power system over long time horizon with the objectives of reducing the operating costs while fulfilling the load requirements. A comprehensive comparative assessment of three distinctive metaheuristic optimizers for solving the DED problem of the standard 30-bus IEEE system is proposed. Marine Predators Algorithm (MPA), Artificial Protozoa Optimizer (APO) and Particle Swarm Optimizer (PSO) are the candidate optimizers under concern. The statistical measures are used to assess the stability and robustness of each technique in consistently obtaining the optimal solution. The results clearly demonstrated the superiority of MPA in achieving the minimum operating cost with remarkably high efficiency, robustness, and stability for both investigated power systems when compared with the other optimization techniques. The statistical analysis further confirmed the consistency and reliability of the proposed method across multiple independent runs and different system dimensions. In addition, the results revealed that the integration of renewable energy sources significantly contributed to reducing both the total operating cost and emission levels, highlighting the important economic and environmental advantages of renewable energy incorporation within modern DED frameworks.

Keywords: Dynamic economic emission dispatch, Renewable energy sources, Statistical measure, Marine predators algorithm , Artificial protozoa optimizer, Particle swarm optimizer.

1. Introduction

In recent years, renewable energy sources (RESs) have experienced rapid integration into power grids worldwide, contributing increasingly to meeting the growing electricity demand [1-4]. Their environmental compatibility, sustainability, and potential to reduce greenhouse gas emissions have made RESs essential components of the transition toward cleaner energy systems. Furthermore, continuous technological advancements, economies of scale, and improvements in manufacturing processes have significantly reduced the costs of RES-based energy projects, thereby enhancing their economic competitiveness [5-9]. Despite these advantages, the operation of RESs is inherently associated with several challenges, particularly the intermittency, weather dependency, and uncertainty of renewable generation. Consequently, effective coordination between conventional fossil-fuel-based generating units and RESs is essential to ensure power supply security, system reliability, economic operation, and long-term sustainability.

In response to these challenges, modern power systems must improve the efficiency of fossil-fuel utilization while accommodating increasing levels of renewable generation under dynamic and uncertain operating conditions. Economic dispatch (ED) represents a fundamental optimization function in power system operation, aiming to optimally allocate the generation output among available generating units while satisfying system demand and operational constraints. Traditionally, ED has focused primarily on minimizing fuel costs; however, the increasing integration of RESs has expanded its objectives to include renewable utilization, emission reduction, operational flexibility, and system reliability [10-12]. Therefore, advanced ED strategies are increasingly required to achieve an optimal balance between economic efficiency, environmental sustainability, renewable energy integration, and secure power system operation.

The integration of renewable energy sources (RESs), particularly solar and wind power, into the economic dispatch (ED) framework can significantly reduce dependence on conventional thermal generating units and their associated operating costs. By increasing the utilization of renewable generation, such integration can also reduce fossil-fuel consumption and consequently mitigate harmful emissions and greenhouse gas releases [13,14]. However, the inherent intermittency and uncertainty of wind and solar generation introduce additional complexity into the ED problem. Renewable power availability varies with meteorological conditions, requiring dispatch strategies to continuously balance fluctuating renewable generation with system demand. Consequently, renewable-integrated ED provides a challenging environment for optimization algorithms, particularly in terms of achieving an appropriate trade-off between economic operation, renewable utilization, and system reliability [15-17]. From a practical standpoint, effective renewable integration can enhance operational flexibility, improve system sustainability, and reduce the overall carbon footprint. Therefore, the incorporation of RESs has evolved from an optional enhancement into an essential component of modern ED frameworks seeking to simultaneously achieve economic efficiency, reliable operation, and environmental sustainability [18–20].

In modern power systems, ED is formulated as an optimization problem that seeks to minimize the total generation operating cost while satisfying the power balance equation, generator operating limits, and relevant network constraints. The increasing penetration of renewable resources, particularly wind and photovoltaic (PV) generation, has substantially increased the complexity of this problem because of their intermittent and uncertain power output. Accordingly, advanced optimization and forecasting techniques are increasingly employed to coordinate conventional generating units with renewable resources. Such coordination enables more efficient utilization of available generation, reduces fuel consumption and operating costs, and contributes to lower greenhouse gas emissions in smart-grid and renewable-integrated power systems.

Recent research on renewable-integrated ED has increasingly focused on stochastic, robust, and hybrid optimization frameworks to account for uncertainties associated with wind speed, solar irradiance, and renewable power availability. These approaches aim to improve the reliability and operational performance of power systems while maximizing renewable energy utilization. In parallel, metaheuristic optimization algorithms have attracted considerable attention because of their ability to solve nonlinear, non-convex, and highly constrained ED problems without requiring strict mathematical assumptions. Algorithms such as the Genetic Algorithm (GA), Particle Swarm Optimization (PSO), Marine Predators Algorithm (MPA), Aquila Optimizer (APO), and their improved or hybrid variants have demonstrated considerable potential for solving complex ED problems involving renewable generation [21–23]. Numerous metaheuristic techniques have been investigated for ED applications [24–26], with substantial differences in their convergence characteristics, computational complexity, exploration–exploitation behavior, and computational burden. In this study, PSO, MPA, and APO are selected as competing optimization approaches for solving the ED problem in different power-system configurations incorporating wind and PV generation.

The Marine Predators Algorithm (MPA) is a population-based metaheuristic optimization technique inspired by the optimal foraging strategies observed in marine predators. Its search mechanism is primarily governed by Brownian and Lévy movement patterns, which enable an effective balance between global exploration and local exploitation. This characteristic makes MPA suitable for complex ED problems characterized by nonlinear cost functions, valve-point loading effects, transmission losses, and multiple generator constraints. Previous studies have reported that MPA can provide competitive convergence characteristics, solution accuracy, and robustness when compared with several conventional and metaheuristic optimization approaches [27-29]. These characteristics motivate its consideration as one of the optimization methods investigated in the present study.

The Aquila Optimizer (APO) is a bio-inspired metaheuristic algorithm designed to emulate the adaptive hunting and foraging behaviors of the Aquila. Through different search strategies, APO provides a dynamic balance between global exploration and local exploitation, allowing it to navigate complex optimization landscapes effectively. In ED applications, APO can be formulated to minimize the total generation cost while satisfying power balance, generator operating limits, transmission-loss requirements, and other system constraints. Its adaptive search mechanism makes it particularly attractive for nonlinear and non-convex ED problems, including those involving valve-point loading effects. Previous investigations have demonstrated the potential of APO to achieve competitive convergence speed, solution accuracy, and robustness in complex optimization problems [28–30].

Particle Swarm Optimization (PSO) is one of the most widely adopted population-based metaheuristic algorithms for power-system optimization. Inspired by the collective behavior of social organisms, PSO iteratively updates the position and velocity of each particle according to its individual best solution and the best solution identified by the entire swarm. This relatively simple search mechanism enables PSO to efficiently address nonlinear and non-convex ED problems while accommodating practical constraints such as generator operating limits, valve-point loading effects, prohibited operating zones, and transmission losses. Numerous studies have demonstrated the effectiveness of conventional and improved PSO variants in achieving accurate solutions with competitive computational efficiency for ED and renewable-integrated power-system applications [30-32]. Owing to its established performance and widespread application, PSO provides an appropriate benchmark against which the more recently developed MPA and APO algorithms can be evaluated.

Although the quality of an optimization algorithm is commonly assessed according to the best operating cost obtained, evaluating a metaheuristic solely on the basis of its best solution may not provide a complete indication of its performance. Since metaheuristic algorithms are inherently stochastic, repeated independent executions may produce different solutions because of variations in their initial populations and search trajectories. Therefore, statistical measures such as standard deviation (SD) and confidence interval (CI) provide important complementary indicators for evaluating the consistency, robustness, and reliability of optimization results [33,34]. A lower SD indicates reduced variability among independent runs and, consequently, greater solution consistency. Similarly, the CI provides an estimate of the uncertainty associated with the obtained performance measure and enables a more statistically meaningful comparison between competing algorithms. The simultaneous consideration of solution quality and statistical variability transforms the assessment from a comparison based solely on the best deterministic result into a statistically supported evaluation of algorithmic performance [33,34]. Accordingly, SD and CI are particularly important for determining whether an algorithm can repeatedly achieve competitive solutions rather than obtaining a favorable result in only a limited number of runs.

Despite the extensive application of metaheuristic optimization techniques to ED with renewable generation, the existing literature provides relatively limited comprehensive statistical assessments of algorithmic performance, particularly regarding the consistency and robustness of the obtained solutions across repeated independent runs and different system configurations [35–38]. In many studies, greater emphasis is placed on reporting the minimum or best operating cost, while the variability of the obtained solutions and the statistical reliability of the optimization process receive comparatively less attention. Consequently, the relative stability and repeatability of different optimization algorithms under varying operating conditions remain insufficiently characterized. This limitation highlights the need for a systematic comparative framework that considers not only the quality of the optimal solution but also the statistical consistency and robustness of the optimization process.

To address this gap, this article presents a comprehensive statistical comparison of three metaheuristic optimization algorithms—PSO, MPA, and APO—for solving the economic dispatch problem in conventional and renewable-integrated power systems. The primary objective is to identify the optimization approach that can consistently achieve low operating costs while maintaining high solution stability and robustness over multiple independent runs. To provide a representative and fair assessment, the proposed comparative framework is applied to power systems with different scales and operating characteristics. The IEEE 6 system benchmark systems is considered because of their widespread use in ED research and their suitability for evaluating the performance of optimization algorithms under different system complexities. Several operating scenarios are investigated, including system operation without renewable generation and operation with integrated wind and PV power plants. For each scenario, the economic and operational performance of the three algorithms is evaluated together with statistical indicators, thereby providing a comprehensive assessment of their solution quality, consistency, and robustness.

The remainder of this article is organized as follows. Section 2 presents the mathematical formulation of the economic dispatch problem, including the objective function and associated operating constraints. Section 3 describes the optimization algorithms considered in the study. Section 4 introduces the investigated IEEE benchmark systems and the renewable-energy configurations. Section 5 presents the proposed simulation and statistical evaluation methodology. Section 6 discusses and compares the obtained results for the different operating scenarios and optimization techniques. Finally, Section 7 summarizes the main findings and presents the conclusions of the study.

2. ED Model

The ED model is generally formulated as a constrained optimization formulation in which the objective is to minimize the total generation cost function, T_C, (Eq. 1). This optimization process seeks to achieve the most efficient allocation of power generation across available units while strictly satisfying all system operating constraints.

2.1 Objective function

The overall generation cost is obtained as the aggregate of the fuel cost for each generator to the emission cost [10].

$$T_C = F_C + \mathrm{E_c} \tag{1}$$

$$F_C = \sum_{i=1}^{N} v_i(P_i)^2 + t_iP_i + u_i \tag{2}$$

$$E_c = h_i * \left(\sum_{i=1}^{N} (x_i(P_i)^2 + y_iP_i + z_i) \right) \tag{3}$$

$$h_i = \frac{F_c(P_{i,max})}{E_T(P_{i,max})} = \frac{\left(v_i(P_{i,max})^2 + t_iP_{i,max} + u_i\right)}{\left(x_i(P_{i,max})^2 + y_i\,P_{i,max} + z_i\right)} \tag{4}$$

where P_i denotes the real power output of generating unit i, while N denotes the number of committed units in the system. The fuel cost component is characterized by the cost coefficients, $v_i, t_i,$ and u_i, whereas the emission cost is governed by the penalty factor h_i in conjunction with the emission coefficients $x_i, y_i,$ and z_i. In addition, $P_{i,max}$ specifies the upper operating limit of the power output for unit [10].

2.2 Constraints

- Power balance constraints

$$\sum_{i=1}^{n} P_i - P_L - P_D = 0 \tag{5}$$

$$P_L = \sum_{i=1}^{N}\sum_{j=1}^{N} P_iB_{ij}P_j + \sum_{i=1}^{N} B_{0i}P_i + B_{00} \tag{6}$$

where P_D denotes the total system load demand, P_L represents the corresponding transmission power losses, and B_{ij}, B_{oi}, B_{oo} are the B-matrix transmission loss coefficients used to model network loss characteristics.

- Generator operating limits constraints

$$P_{i,\min} \leq P_i \leq P_{i,max}; i = 1, \dots, N \tag{7}$$

where $P_{i,\min}$, $P_{i,max}$ denote the lower and upper bounds of the power output of generating unit i, respectively [10,39,40].

3. Optimizers under concern

3.1. MPA

The MPA is a nature-inspired metaheuristic optimization technique that emulates the foraging behavior of marine predators. It is primarily driven by Lévy and Brownian motion-based movement strategies and has demonstrated strong effectiveness across a wide range of engineering and scientific optimization problems [39-42]. The MPA framework is generally divided into three main phases, as described below:

Exploration phase: This phase occurs during the initial one-third of the iterations, where a high velocity ratio is assumed. In this stage, the prey exhibits stochastic movement governed by Brownian motion, which promotes global exploration of the search space and leads to the following position updating rules [41,42]:

$$\overrightarrow{step\_size_i} = \overrightarrow{R_B} \otimes \left(\overrightarrow{E_i} - \overrightarrow{R_B} \otimes \overrightarrow{Prey_i}\right) \tag{8}$$

$$\overrightarrow{Prey_i} = \overrightarrow{Prey_i} + P \times \vec{R} \otimes \overrightarrow{step\_size_i} \tag{9}$$

where P=0.5, $\vec{R}$ is a uniformly distributed random vector in [0,1], and $\overrightarrow{R_B}$ is a normally distributed random vector modeling Brownian motion. Moreover, E_i denotes the elite matrix guiding the search toward promising regions of the solution space.

Intermediate phase: This phase occurs during the middle one-third of iterations under an equal velocity ratio. The population is split equally into exploration and exploitation groups (50% each), and the first half is updated using the following rule [13,41,42]:

$$\overrightarrow{step\_size_i} = \overrightarrow{R_L} \otimes \left(\overrightarrow{E_i} - \overrightarrow{R_L} \otimes \overrightarrow{Prey_i}\right) \tag{10}$$

$$\overrightarrow{Prey_i} = \overrightarrow{Prey_i} + P \times \vec{R} \otimes \overrightarrow{step\_size_i} \tag{11}$$

The remaining 50% of the population is updated using the following procedure [13,31,32]:

$$\overrightarrow{step\_size_i} = \overrightarrow{R_B} \otimes \left(\overrightarrow{R_B} \otimes \overrightarrow{E_i} - \overrightarrow{Prey_i}\right) \tag{12}$$

$$\overrightarrow{Prey_i} = \overrightarrow{E_i} + P \times CF \otimes \overrightarrow{step\_size_i} \tag{13}$$

$$CF = \left(1 - \frac{itr}{Maxitr}\right)^{\left(\frac{2 \times itr}{Maxitr}\right)} \tag{14}$$

where $\overrightarrow{R_L}$ is generated based on Lévy flight principles. The CF adaptively regulates the step size within the MPA. Here, itr denotes the current iteration, while $Maxitr$ represents the maximum number of iterations.

Exploitation phase: This phase takes place during the final one-third of iterations under a low velocity ratio. In this stage, prey movement is governed by Lévy motion, resulting in the following update equations [13,41,42]:

$$\overrightarrow{step\_size_i} = \overrightarrow{R_L} \otimes \left(\overrightarrow{R_L} \otimes \overrightarrow{E_i} - \overrightarrow{Prey_i}\right) \tag{15}$$

$$\overrightarrow{Prey_i} = \overrightarrow{E_i} + P \times CF \otimes \overrightarrow{step\_size_i} \tag{16}$$

Marine predators are strongly affected by Fish Aggregating Devices (FADs), spending most of their time near them due to high prey density. In the remaining time, they undertake long-range exploratory movements across different directions to search for widely dispersed prey. The influence of FADs can be mathematically formulated as follows [13,41,42]:

$$\overrightarrow{Prey_i} = \begin{cases} \overrightarrow{Prey_i} + CF\left[\overrightarrow{X_{mn}} + \vec{R} \otimes \left(\overrightarrow{X_{mx}} - \overrightarrow{X_{mn}}\right)\right] \otimes \vec{U}, & if \;\; r \le FADs \\ \overrightarrow{Prey_i} + \left[FADs\,(1-r) + r\right]\left(\overrightarrow{Prey_{r1}} - \overrightarrow{Prey_{r2}}\right), & if \;\; r > FADs \end{cases} \tag{17}$$

$FADs$ = 0.2 represents the degree of influence of Fish Aggregating Devices on the optimization process. $\vec{U}$ is a binary vector consisting of 0 and 1 values, while r is a uniformly distributed random variable in [0,1]. X_{mx} and X_{mn} denote the upper and lower bounds of the decision variables, respectively. $Prey_{r1}$ and $Prey_{r2}$ are randomly selected individuals from the prey matrix. Figure 1 presents the flowchart describing the main steps of the MPA implementation [13,41,42].

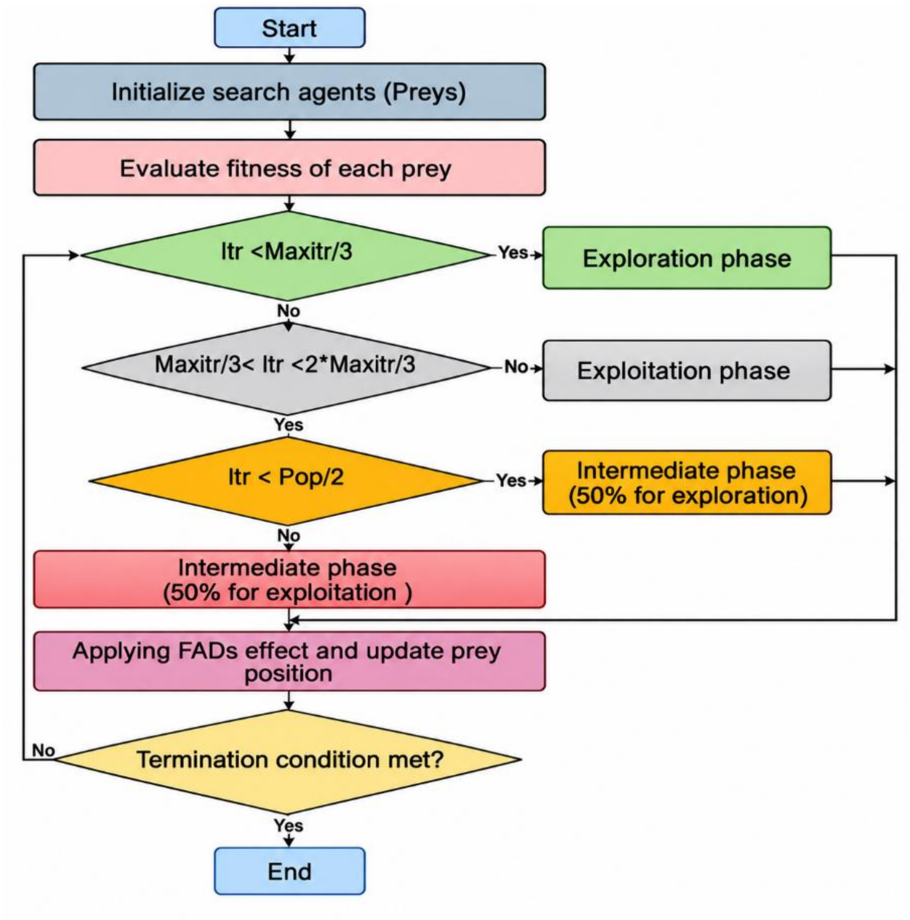

Figure 1. Flow chart of MPA [13].

3.2. *APO*

The APO replicates the intelligent adaptive mechanisms of protozoa by integrating chemotactic sensing, pseudopodal mobility, and feedback-driven learning to efficiently explore complex optimization landscapes. The algorithm is composed of four fundamental stages: initialization, exploration, exploitation, and adaptive adaptation [43-45].

Initialization Phase: In this phase, each protozoan represents a candidate solution in continuous search space. The initial positions are randomly and uniformly initialized within the predefined problem bounds [43-45]:

$$X_i = LB + r(UB - LB) \tag{18}$$

where LB and UB denote the lower and upper bounds, and r ∈[0, 1] is a uniform random variable.

Exploration Phase (Global Search): During this phase, protozoa traverse the search space by combining gradient-informed movement with stochastic perturbations to enhance diversity and prevent premature convergence. The chemotactic update rule is defined as [43-45]:

$$\Delta X_i = \beta . \nabla f(X_i) + \gamma . N(0,1) \tag{19}$$

where $\nabla f(X_i)$ is the objective gradient at X_i, β controls gradient-driven movement, γ scales stochastic noise, and $N(0,1)$ is a standard Gaussian vector.

Pseudopodal exploitation Phase: In this phase, APO intensifies exploitation through a pseudopodal contraction mechanism that drives agents toward the current global best solution. The position update is formulated as [43-45]:

$$X_i(t+1) = X_i(t) + r(t).\left(X_{best} - X_i(t)\right) \tag{20}$$

$$r(t) = r_0.\left(1 - \frac{t}{T}\right) \tag{21}$$

X_{best} denotes the best solution identified by the population, whereas $r(t)$ is a time-varying contraction coefficient defined by the initial value r_0, the current iteration t, and the maximum iterations T [43-45].

Adaptive learning: In this phase, APO incorporates a feedback-driven learning mechanism to replicate adaptive behavior based on historical movements. Each protozoan updates its position by utilizing the deviation from its previous state [43-45]:

$$X_i \leftarrow X_i + \lambda.(X_i - X_i^{prev}) \tag{22}$$

Here, X_i^{prev} denotes the previous location of agent i, and λ is a learning coefficient that regulates the influence of historical movement. This mechanism reinforces effective search directions while diminishing unproductive exploration.

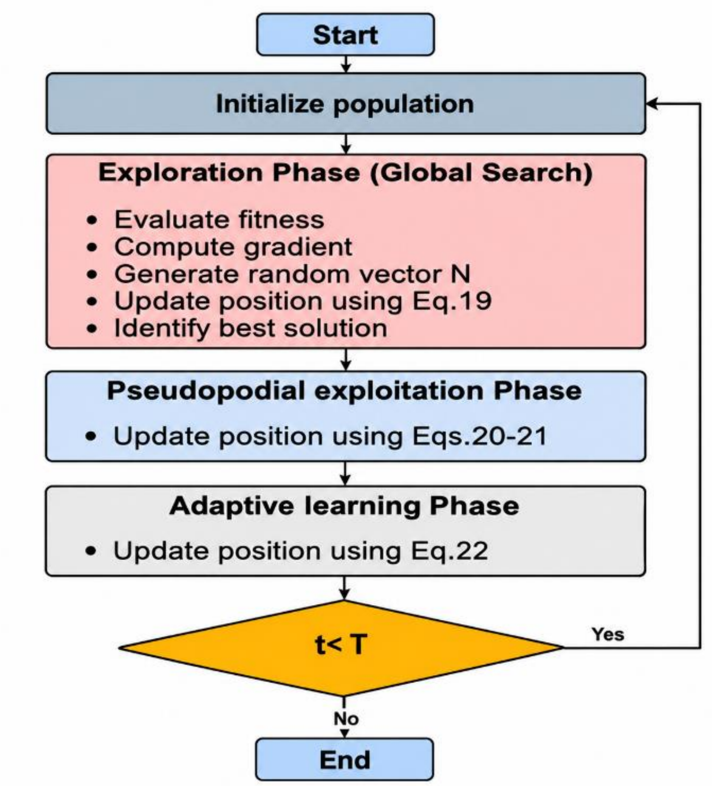

Figure 2. APO flow chart [45].

3.3. *PSO*

PSO enjoys simplicity, exhibits rapid convergence, and requires fewer parameters and computational resources than GA. The versatility and speed of PSO promote it as an appealing approach for addressing intricate optimization challenges, including those characterized by multiple local optima, fluctuating objective functions, or high-dimensional spaces [30-32]. In PSO, particles explore the search space to find the optimal solution by updating their positions based on individual and collective experiences, using specific velocity and position equations. The velocity and position updates are mathematically defined as follows (23) and (24):

$$V_i(r+1) = w_t * V_i(r) + C_1 rd_1 \left(P_{best,i} - X_i(r)\right) + C_2 rd_2 (g_{best} - X_i(r)) \tag{23}$$

$$X_i(r+1) = X_i(r) + V_i(r+1) \tag{24}$$

The flow chart of PSO is shown in Figure 3.

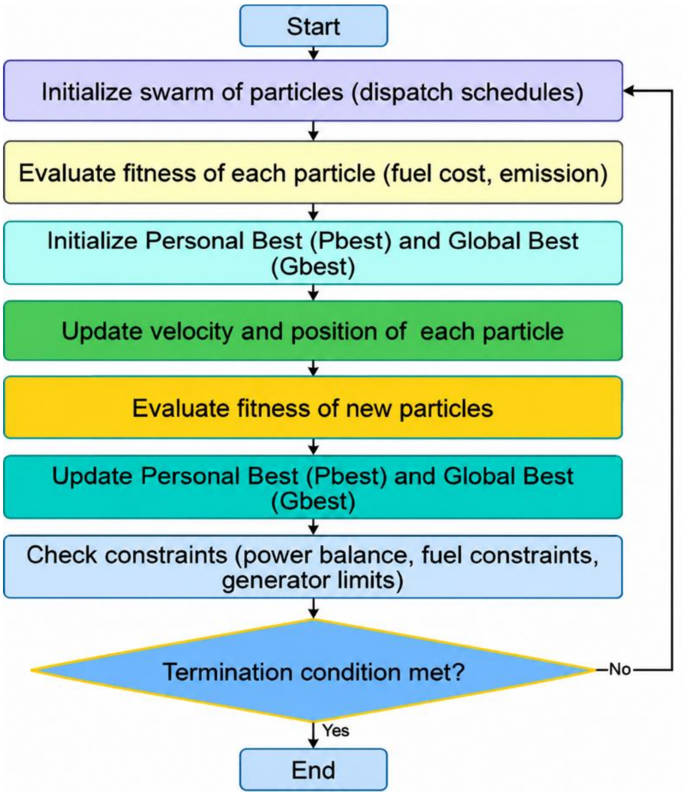

Figure 3. PSO flow chart [31]

4. Case study

The system under concern is 30 bus, six-unit IEEE power system as shown in, Figure 4. The parameters of the 6-unit generating system are presented in Table 1, while the corresponding loss coefficients are listed in Table 2 [21,22].

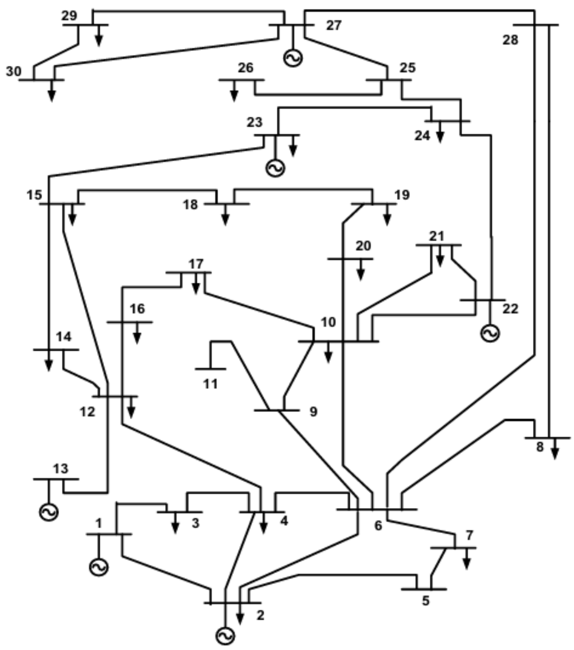

Figure 4. Standard 30-bus six machine IEEE power system.

Table 1. Generating unit test data of the 6-unit system [33].

Gen. unit	v_i (\$/MW^2.h)	t_i (\$/MW .h)	u_i (\$/h)	x_i (\$/MW^2.h)	y_i (\$/MW .h)	z_i (\$/h)	$P_{i,min}$ (MW)	$P_{i,max}$ (MW)
1	0.1525	38.54	756.8	0.0042	0.33	13.86	10	125
2	0.106	46.16	451.32	0.004	0.33	13.86	10	150
3	0.0208	40.159	1049.99	0.00683	-0.5455	40.27	35	225
4	0.0355	38.31	1234.5	0.0068	-0.5455	40.27	35	210
5	0.0211	36.328	1658.6	0.0046	-0.5112	42.7	130	325
6	0.0179	38.27	1356.7	0.0042	-0.5112	42.7	125	315

Table 2. Parameters of transmission loss for 6-unit system [33].

B-loss coefficient					
0.14E-04	**0.17E-04**	**0.15E-04**	**0.19E-04**	**0.26E-04**	**0.22E-04**
0.17E-04	0.60E-04	0.13E-04	0.16E-04	0.15E-04	0.20E-04
0.15E-04	0.13E-04	0.65E-04	0.17E-04	0.24E-04	0.19E-04
0.19E-04	0.16E-04	0.17E-04	0.71E-04	0.30E-04	0.25E-04
0.26E-04	0.15E-04	0.24E-04	0.30E-04	0.69E-04	0.32E-04
0.22E-04	0.20E-04	0.19E-04	0.25E-04	0.32E-04	0.85E-04

The load demand of the 6-unit IEEE power system under consideration is shown in Figure 5 for 24h.

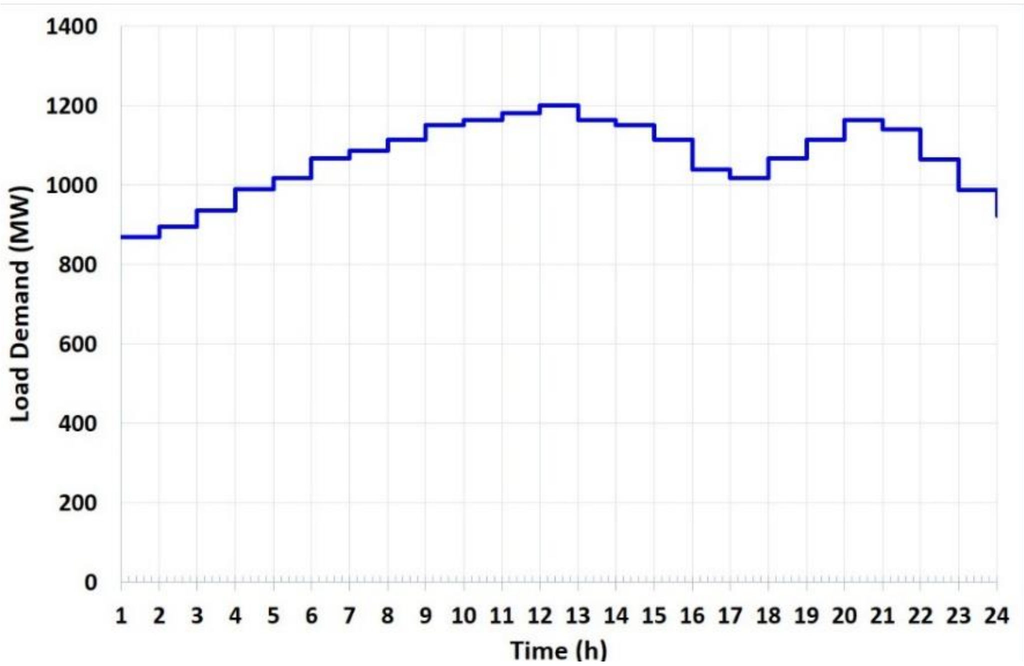

Figure 5. Load demand for 6-unit IEEE power system

Figure 5 shows that the system experiences a peak during 12AM of 1200MW. The integration of RESs would possibly reduce the dependency on fossil fuel power plants. This utlimately achieves double goals

1. reduces the running costs of the power system
2. decreasing the level of the pollution.

The harvested power from PV and wind power plant in the system under consideration are shown in Figure 6.

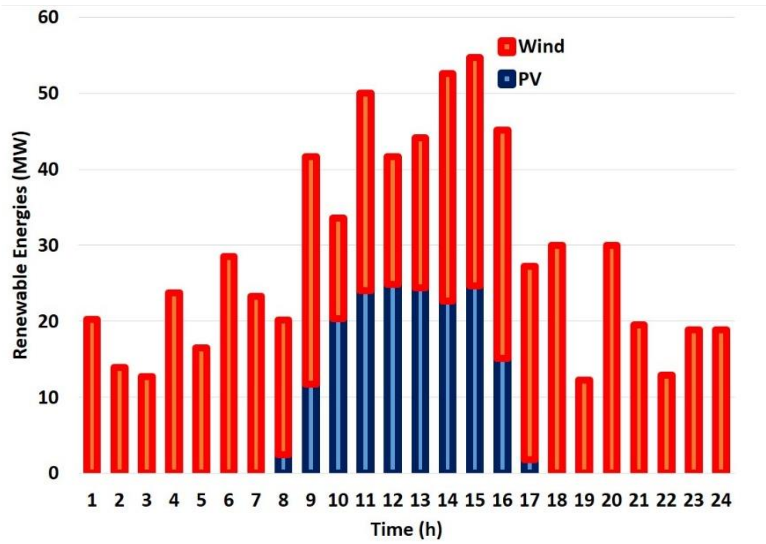

Figure 6. Powers of PV(blue), wind (red).

Figure 6 shows that the majority of RESs is due to the wind energy, where the PV contributes only for 10 hours during the day. The solar irradiance is assumed to vary along the day. Moreover, the average wind speed is assumed to vary.

- *Methodology*

The study methodology consists of two phases:

- Phase 1: Comprehensive comparison between APO, MPA, and PSO.
- Phase 2: Validation of the proposed DEED framework under diverse operating scenarios with and without RES using the highest-performance optimization algorithm.

To determine the most reliable and high-performing optimizer among MPA, APO, and PSO, a comprehensive performance assessment is conducted on the studied systems under a 1000 MW load demand. The comparative evaluation examines the capability of each optimizer to satisfy the required load while achieving the minimum Total Cost (TC), thereby reflecting both solution quality and operational effectiveness. In addition to cost-based performance, the assessment incorporates several statistical indicators, including SD, CI analysis, CI width, and average computational time. These metrics are obtained over 50 independent runs for each optimizer, ensuring a sufficiently large sample for dependable estimation of mean performance and statistically meaningful comparison.

SD is a statistical measure that captures the extent of data dispersion around the mean, indicating the level of consistency within a dataset. Lower SD values denote higher stability and uniformity, while higher values reflect greater variability and deviation [13]. It is mathematically defined as follows:

$$SD = \sqrt{\frac{1}{n-1}\sum_{d=1}^{n}(\bar{x} - x_d)^2} \tag{25}$$

$$\bar{x} = \frac{1}{n}\sum_{d=1}^{n} x_d \tag{26}$$

where x_d denotes the individual data points in the dataset, $\bar{x}$ represents the arithmetic mean of all observations, and n is the total number of samples [13].

The CI specifies a statistical range estimated from sample data within which the true population mean is likely to lie, subject to a chosen confidence level (e.g., 95%). It serves as an indicator of how precisely the sample mean represents the underlying population value [13]. The CI is mathematically formulated as follows:

$$CI = \bar{x} \pm Z * \left(\frac{SD}{\sqrt{n}}\right) \tag{27}$$

Z represents the critical value derived from the standard normal distribution, determined according to the selected confidence level [13].

The best optimizer is selected based on cost performance, stability, and computational efficiency. A low SD and narrow CI indicate consistent convergence and robust solution quality across runs.
In Phase 2, four distinct operating scenarios are investigated to assess the performance of the proposed DEED framework under conditions with and without RES integration. These scenarios are defined as follows:

- Scenario 1: DEED without RES integration for the 6-unit system, optimized using MPA.
- Scenario 2: DEED with RES integration for the 6-unit system, optimized using MPA.

5. Results and Discussion

5.1 MPA versus APO and PSO

Simulations were performed in MATLAB on an Intel Core i7 (16 GB RAM) system. All optimizers used 50 population size and 1000 iterations. In PSO, $C1$ and $C2$ were tuned in [1.5–2.5] and set to 1.5, while inertia weight was selected as 0.7 from [0.4–0.9]. Other parameters remained unchanged for fairness. Tables 3 presents the total cost and optimal power dispatch for the 6-unit under a 1000 MW load. Table 3 and Table 4 summarizes the performance metrics (SD, CI, and execution time) of APO, MPA, and PSO over 50 runs .

Table 3. Power allocation of each unit to meet a load demand of 1000 MW.

Method	P_1(MW)	P_2(MW)	P_3(MW)	P_4(MW)	P_5(MW)	P_6(MW)	P_L(MW)	TC ($)
PSO	84.68	92.47	183.87	163.38	259.06	250.94	34.4	94827.12
APO	89.68	92.03	184.15	158.45	260.05	249.94	34.3	94843
MPA	85.27	92	184.64	163.3	259.47	249.7	34.38	94826.3

Table 4. Statistical results for APO, MPA, and PSO over 50 runs at 1000 MW.

Method	SD	CI	CI Width	Time (s)
PSO	0.49	[94826.98, 94827.26]	0.28	1.83
APO	218.36	[94890.61, 95014.73]	124.12	0.89
MPA	1.47E-11	[94826.30, 94826.30]	0	2.28

Table 3 indicates that both MPA and PSO outperform APO in terms of optimization quality, achieving an approximate reduction of 0.02% in the overall operating cost. This enhancement can be attributed to their stronger capability to effectively explore complicated search spaces, escape premature convergence to local optima, and obtain more optimal solutions.

As demonstrated in Table 4, MPA delivers the highest level of robustness and reliability, as reflected by the CI width. The CI associated with MPA is significantly smaller, reaching nearly 100% lower values compared with APO and PSO. In addition, MPA records an almost 100% decrease in standard deviation relative to APO and PSO, highlighting its highly consistent convergence behavior across repeated runs. The superior stability of MPA stems from its well-regulated population update mechanism and carefully balanced exploration process, which support precise convergence toward the global optimum region. Nevertheless, the enhanced search capability of MPA comes at the expense of higher computational effort. The execution time of MPA is approximately 51.37% greater than that of PSO because of the increased complexity of its search procedures. Despite this, MPA still achieves about a 60.96% reduction in computational time compared with APO.

Table 3 demonstrates that MPA achieves superior optimization performance compared with both APO and PSO, leading to reductions in the total operating cost of approximately 0.31% and 0.01%, respectively. This improvement is mainly associated with the enhanced exploration capability of MPA, which allows it to efficiently investigate complex search regions, avoid entrapment in local optima, and attain solutions of higher quality.

Furthermore, as presented in Table 4, MPA exhibits the highest degree of robustness and convergence stability, as indicated by the CI width. The CI values obtained by MPA are approximately 98.2% and 99.97% lower than those achieved by APO and PSO, respectively. In addition, the standard deviation produced by MPA is reduced by nearly 98.19% and 99.97% relative to APO and PSO, respectively, confirming its highly consistent performance over multiple independent runs. The remarkable stability of MPA can be attributed to its accurately regulated population movement strategy and well-balanced exploration mechanism, which facilitate reliable convergence toward the optimal search regions. Nevertheless, the improved search effectiveness of MPA is accompanied by increased computational complexity. Consequently, the execution time of MPA is approximately 52.38% higher than that of APO and about 68.75% greater than that of PSO.

Table 3 and Table 4 indicate that APO and PSO achieve lower computational times than MPA. Nevertheless, both methods still suffer from noticeable instability and inconsistency, as clearly reflected by the SD and CI values. The computational efficiency of MPA can be further improved by decreasing either the population size or the maximum number of iterations.

Although the reported cost reductions of 0.02%, 0.01%, and 0.31% may appear relatively small, these improvements correspond to a 1000 MW load demand, which represents less than half of the total hourly generation capacity of the system. When such savings are extended to higher loading conditions or accumulated over continuous daily operation, they translate into considerable economic benefits over long-term operating horizons. Under conditions of fuel scarcity and continuously increasing fuel prices, even slight reductions in operating cost become highly valuable. Furthermore, the substantial reductions achieved in both SD and CI demonstrate the superior stability, repeatability, and predictability of MPA, thereby providing system operators with lower operational uncertainty and more dependable scheduling decisions.

The comparative evaluation of MPA, APO, and PSO has also been performed under multiple loading scenarios, where the obtained outcomes remain highly consistent with the results reported in Table 3 and Table 4. Accordingly, MPA can be considered the most effective overall optimization technique among the compared approaches in terms of solution quality, robustness, and reliability.

5.2 DEED for 6-Unit IEEE with/without RESs via MPA

Tables 3 and 4 identify that MPA is the best candidate optimizer for the 30 bus 6-unit IEEE system. Therefore, the dynamic economic dispatch for 6-unit IEEE with and without RESs is investigated by MPA only. The results for the different power units in the system over the 24h are illustrated in the following figures.

Firstly the results obtained for the DEED problem of the 6-unit power system without RES integration using the MPA are combined with those for the system with integrating RES. The optimization process aims to determine the optimal power generation schedule for all generating units while satisfying the load demand and operational constraints over the scheduling horizon. The obtained results are analyzed in terms of total operating cost, emission level, and power balance satisfaction. Fig.7 demonstrates the capability of the proposed DEED model to accurately satisfy the power balance constraint, where the total generated power matches the sum of the load demand and system power losses throughout the scheduling period.

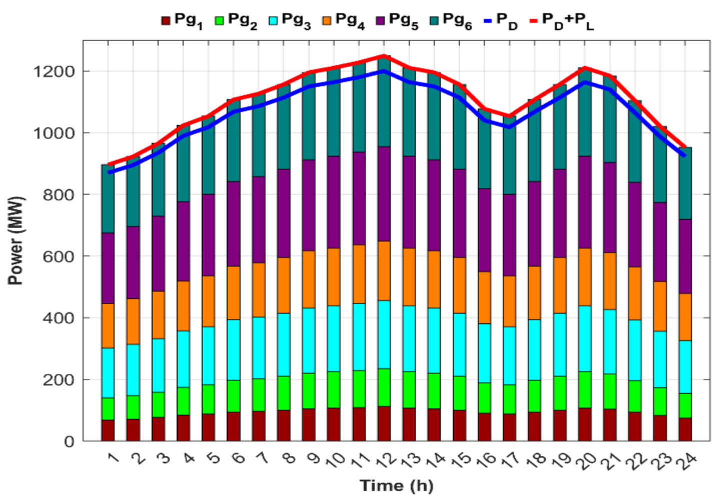

Figure 7. Detailed hourly optimal power generation scheduling and corresponding load demand without RESs for 6-unit IEEE system.

Figure 7 demonstrates the capability and efficiency of the six generating units in maintaining power balance by supplying the required power demand and system losses over the 24-hour scheduling period with high accuracy and without any power deficiency. It can also be observed that the output power of Units 5 and 6 increases by up to 48.8%, which is mainly attributed to their lower generation costs compared with the other generating units, making them more economically favorable during the optimization process.

The results of integrating RESs into the 6-unit power system to reduce the operating cost and emissions resulting from the power generation process are shown in the following. Accordingly, a wind power plant and a solar PV power plant are incorporated into the system, assuming their maximum available generation throughout the day. The remaining required demand is then supplied by optimally dispatching the thermal generating units while satisfying all operational constraints and maintaining the power balance condition. This integration strategy enhances the overall economic and environmental performance of the system by reducing the dependency on conventional thermal generation and improving the utilization of clean energy resources. Figure 8 illustrates a comprehensive representation of the optimal power generated by all units to satisfy the system load demand and transmission loss requirements.

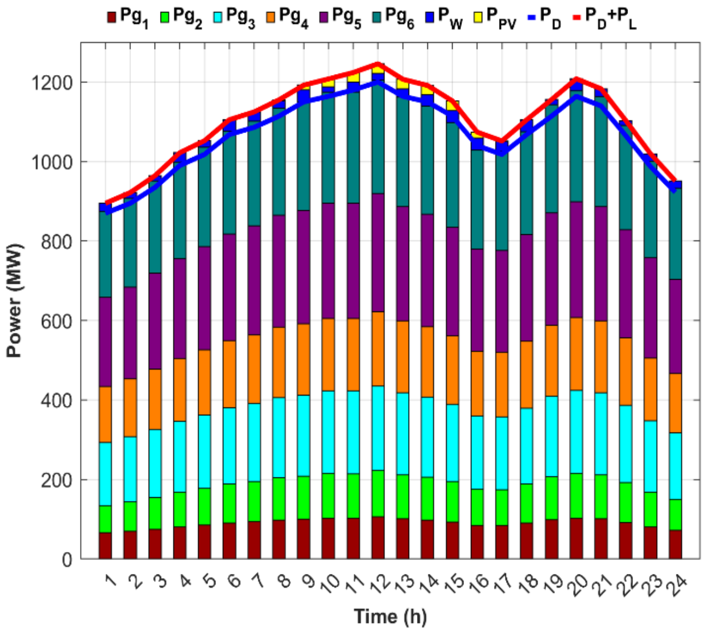

Figure 8. Detailed hourly optimal power generation scheduling and corresponding load demand with RESs for 6-unit IEEE system.

Figure 8 demonstrates the capability of the six generating units with the integration of renewable energy sources to efficiently satisfy the required load demand and system losses over the 24-hour period. The renewable energy contribution accounts for approximately 2.6% of the total required power, which consequently reduces the power generation from the thermal units. For instance, the output power of Units 5 and 6 decreases by about 47.8% compared with the previous scenario without RES integration. Despite these variations in generation levels, the system remains fully capable of meeting the hourly demand while maintaining secure and balanced operation throughout the entire scheduling horizon. The power of unit#1 with and without RESs over the 24 h is shown in Figure 9 for the 6-unit IEEE system via MPA.

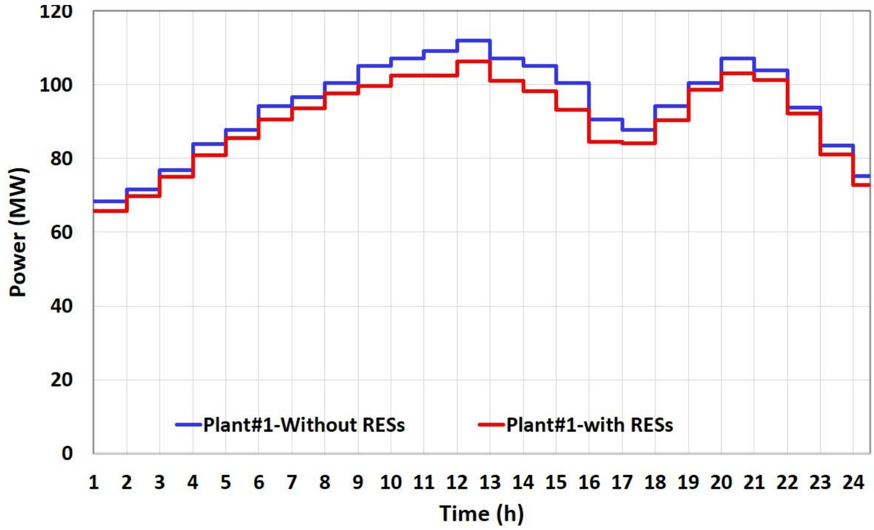

Figure 9. Power of unit#1 with and without RESs.

Figure 9 illustrates the output of generator#1 during the 24 h while the DEED is used to optimize the running costs of the energy. The system is optimized using MPA. Fig. 9 shows that the operation with RESs lowering the output of the generator#1 over the 24h. The RESs as shown in Figure 9 could results in reduction in the output power of unit#1 by around 9% during the periods 12-16 h. The powers of plant#2 over the 24h with and without RESs, while the 6-unit IEEE is optimized using MPA for the DEED are shown in Figure 10.

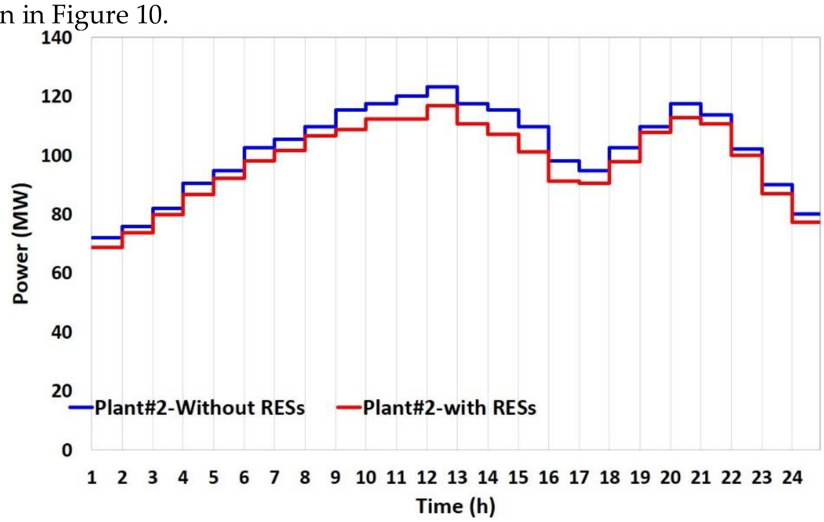

Figure 10. Power of unit#2 with and without RESs.

Figure 10 shows the output of generator#2 during the 24 h while the DEED is used to optimize the running costs of the energy. The system is optimized using MPA. Fig. 10 like Fig. 9 shows that the operation with RESs lowering the output of the generator#2 over the 24h. The RESs as shown in Fig. 10 could results in reduction in the output power of unit#2 by around 9% during the periods 9-16 h.

Comparing Figure 9 and Figure 10 shows that unit#2 is bigger than unit#1. Moreover, its load share is ultimately bigger. Therefore, the RESs for unit#2 have more impact than unit#1. The powers of plant#3 with and without RESs throughout 24 h for the 6-unit IEEE optimized using MPA in the DEED are shown in Figure 11. Plant#3 is considered from the big machines in the system.

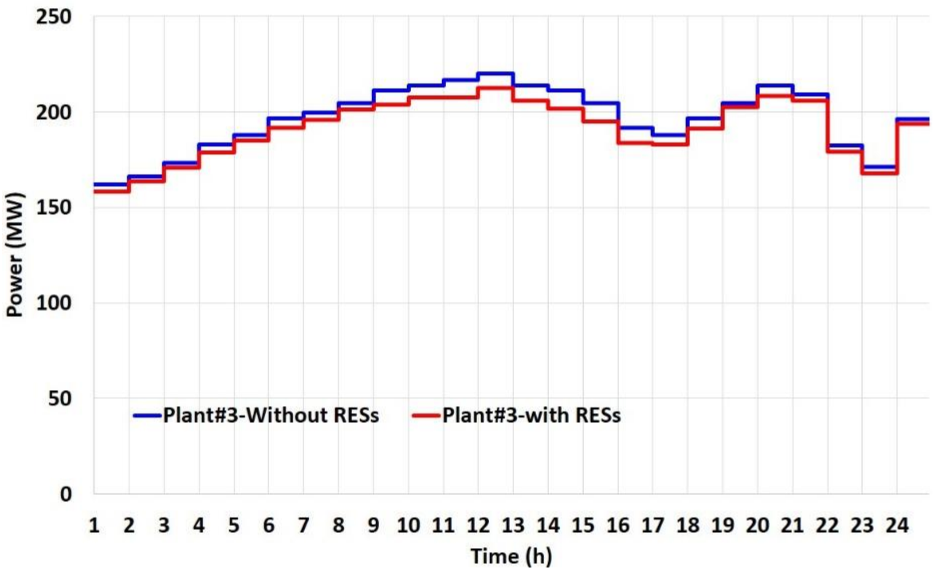

Figure 11. Power of unit#3 with and without RESs.

Figure 11 presents the power of generator#2 during the 24 h while the DEED is used to optimize the running costs of the energy. The DEED is implemented using MPA for the case under consideration. Again, Fig. 11 shows that the RESs results in reduction of output power of unit#3 like unit#1 Fig. 9 and unit#2 Fig. 10. The reduction of the unit#3 could reach 5% during the period from 9-18 h. The reduction in the power of unit#3 is lower than that of units 1&2. This is attributed to the size of unit#3, which is much bigger than that of units 1&2.

Comparing Figure 3, Figure 10, and Figure 11 shows that unit#3 is bigger than units#1 and 2. Moreover, its load share is ultimately bigger. The powers of plant#4 with and without RESs throughout 24 h for the 6-unit IEEE optimized using MPA in the DEED are shown in Figure 12. Plant#4 is considered from the big machines like unit#3 in the 6-unit IEEE system.

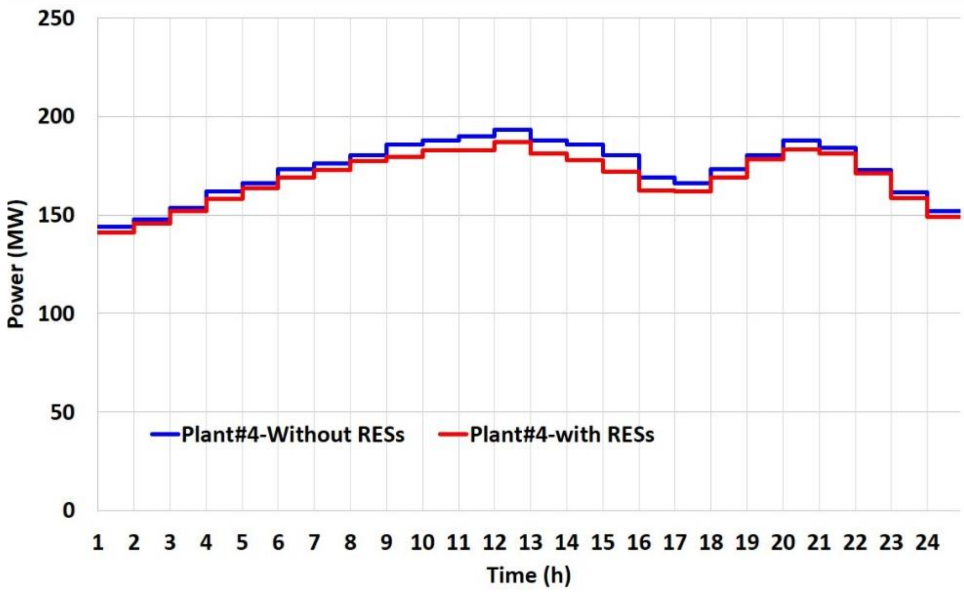

Figure 12. Power of unit#4 with and without RESs.

Figure 12 illustrates the output of unit#4 during the 24 h while the energy cost and emission of the 6-unit IEEE system is dynamically optimized using MPA. The DEED is implemented using MPA for the case under consideration. Again, Figure 12 reveals that the RESs improve the performance of the system under concern. The integration of RESs results in reduction of output power of unit#4 like units#1, 2 and 3. The reduction of the unit#3 could reach 6% during the period from 9-18 h. The reduction in the power of unit#4 is lower than that of units 1&2. This is attributed to the size of unit#4, which is much bigger than that of units 1&2.

The powers of plant#5 with and without RESs throughout 24 h for the 6-unit IEEE optimized using MPA in the DEED are shown in Figure 13. Plant#5 is considered from the big machines in the system.

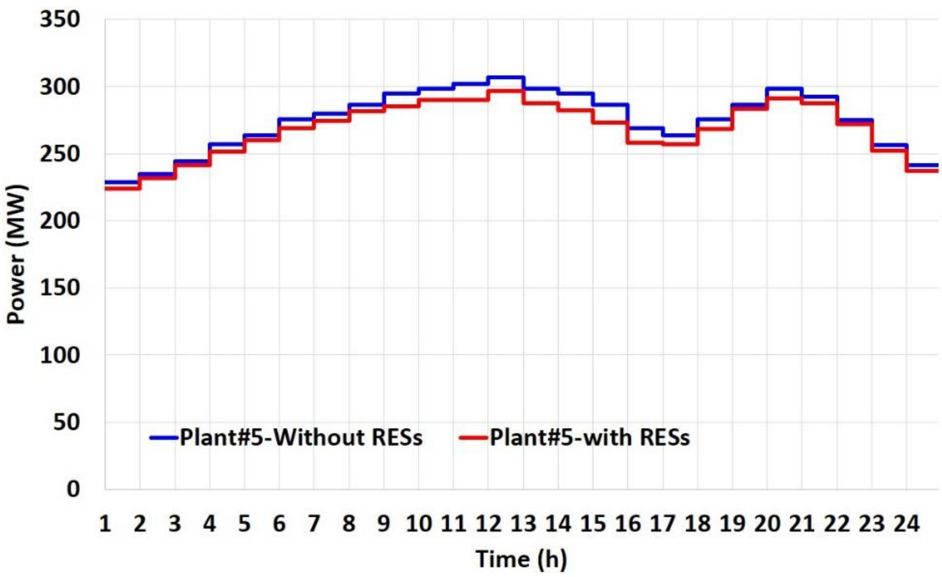

Figure 13. Power of unit#5 with and without RESs.

Figure 13 shows the output of unit#5 during the 24 h while the energy cost and emission of the 6-unit IEEE system are optimized using MPA. MPA is used within the dynamic ED. Again, Figure 13 reveals that the RESs improve the performance of the 6-unit IEEE. The power from unit#5 is reduced during the 24 h. This ultimately reduces the operating cost, emission and losses. The integration of RESs results in reduction of output power of unit#5 like units#1-4. The reduction of the unit#5 could reach 3.4% during the period from 9-18 h. The reduction in the power of unit#5 is lower than that units#1-4. Unit#5 as shown in Figure 13 produces more power than units#1-4, Figs. 3-9-3.12.

The powers of plant#6 with and without RESs throughout 24 h for the 6-unit IEEE optimized using MPA in the DEED are shown in Figure 14. Plant#6 is considered from the big machines in the system.

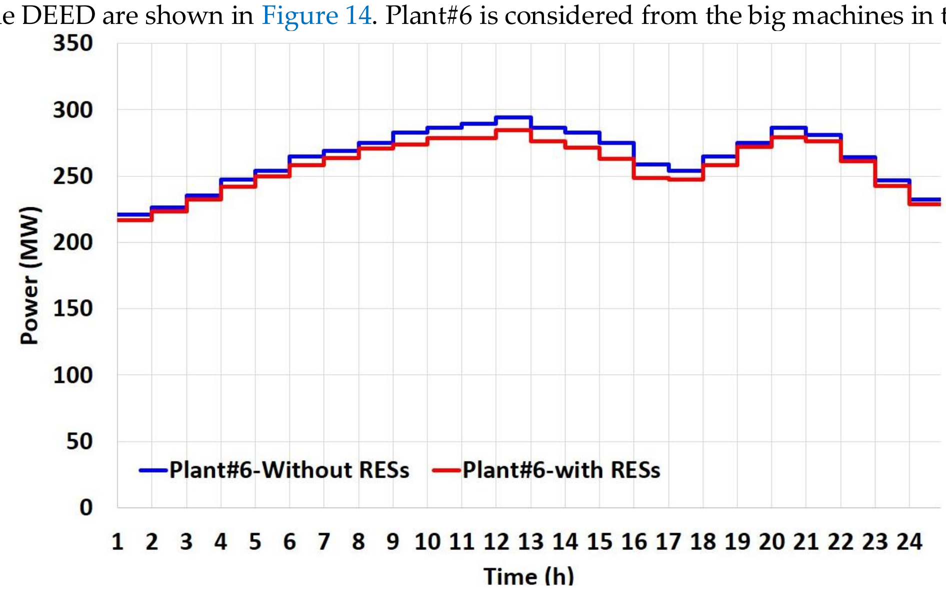

Figure 14. Power of unit#6 with and without RESs.

Figure 14 illustrates the power of unit#6 over the time horizon under concern; The figure shows the power from the unit for the operation of 6-unit IEEE with and without RESs. The energy cost and emission of the 6-unit IEEE system is dynamically optimized DEED via MPA. The integration of RESs into the 6-unit IEEE reduces the output power of unit#6 throughout the 24h. The size of unit#6 is the largest in the 30-bus 6-unit IEEE power system. Thus, the percentage of the reduction in the generated power due to RESs in unit#6 is lower than units#1-5.

6. Energy Management for 6-Unit IEEE with RESs versus without

Figs. 7 to 14 reveal the results of the 6-unit IEEE power system with and without RESs. The results include the power from each unit individually and from the entire system. Moreover, the results include the total system losses during the time span under concern and the load demand. The results clearly validate the ability of the proposed economic dispatch model in fulfilling the system load demand and losses with high reliability and accurate power balance, while reducing the overall operating cost at each hour in the time horizon under concern. Figure 9-14 show that the power is from each individual unit. This is to identify the effectiveness of incorporating RESs into the 30-bus 6-unit IEEE. The comparison between the performance of the 30-bus 6-unit IEEE with and without RESs is extended to the system losses, which is shown on Figure 15.

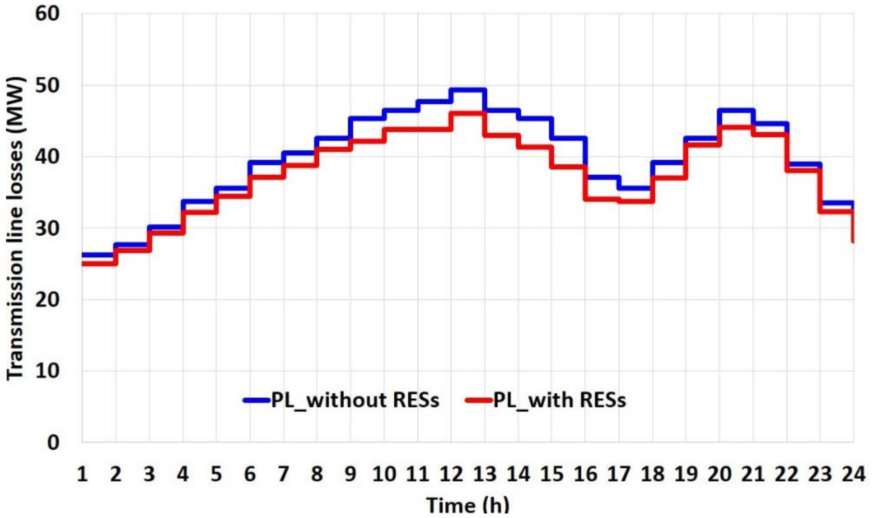

Figure 15. Transmission losses for 6-unit IEEE power without (blue) and with (red) RESs.

Figure 15 shows that the operation of the 6-unit IEEE power system with RESs results in reducing the transmission losses. This could be due to the sites of the renewable power plants. Fig.15 shows that the losses vary according to the load level and the contribution of RESs in reducing the transmission losses varies also with the load level with highest reduction of 6.25%. The variation of the emissions throughout 24h for the 6-unit IEEE power system, while the running cost is determined from DEED via MPA optimizer is shown in Figure 16.

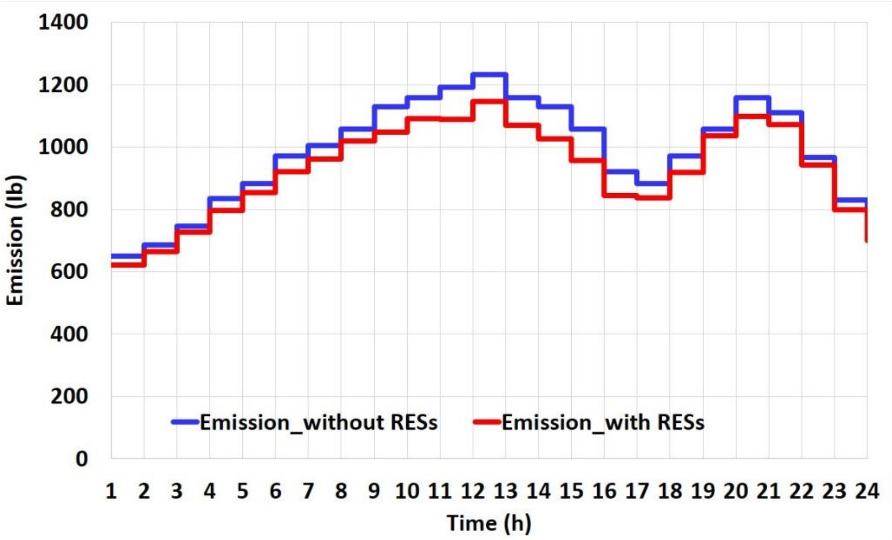

Figure 16. Emission for 6-unit IEEE power without (blue) and with (red) RESs.

DEED effectively decreases the emission, Fig.16. This validates the efficiency and the consistency of the proposed DEED via MPA optimizer, Fig.16. However, despite this technical effectiveness of the MPA comparing with the optimizers under concern PSO and APO, it is essential to further investigate the economic and environmental performance of the system. This includes evaluating the cost-effectiveness of the operation as well as assessing the environmental benefits associated with integrating renewable energy sources. Therefore, a comprehensive analysis is required to examine the feasibility and overall impact of renewable energy integration within the economic dispatch framework.

Table 5 presents a comparative analysis of the total operating cost and the corresponding emissions over the 24-hour scheduling period for 6-unit IEEE power system with and without RESs. This comparison highlights the impact of each case on both economic and environmental performance, allowing for a clear evaluation of the effectiveness of the proposed optimization approach and the integration of renewable energy sources in reducing cost and emissions while maintaining reliable system operation.

Table 5. Total Cost and Emission for 6-unit IEEE.

Scenario	**TC** ($)	**E** (lb)
Without RESs	2520974.26	23523.56
With RESs	2417937.674	22241.32

The integration of RESs into the 30-bus 6-unit IEEE power system results in a noticeable improvement in system performance compared with the operation without RES, where the total operating cost is reduced by approximately 4.3%, while the emission level is decreased by about 6%. These improvements are mainly attributed to the displacement of a portion of thermal generation by clean energy resources, which reduces both fuel consumption and environmental impact.

Overall, the comparative results clearly indicate that increasing the share of RES significantly contributes to improving system performance by simultaneously reducing operational costs and emissions while maintaining secure and reliable power supply.

Table 3 to Table 5 indicate that the MPA is the most promising optimizer in the optimizers under concern: PSO and APO. This meta-heuristic optimizer results in reduced standard deviation and interval of confidence. Moreover, the MPA results in the minimum operating cost for the 6-unit IEEE power system. The comprehensive statistical comparison evaluates and validates the superiority of the proposed MPA approach in terms of solution quality, stability, and computational performance. Furthermore, the effectiveness of the proposed MPA method was tested on 6-unit IEEE power system to ensure the robustness and consistency of the obtained results. Subsequently, DEED was investigated over a 24-hour scheduling horizon, considering scenarios with and without RES integration, with the aim of minimizing both total operating cost and emission levels.

Figure 7 to Figure 16 demonstrated the efficiency of MPA and its ability to achieve the lowest operating cost with high stability for the two scenarios of 6-unit IEEE power system. In addition, the DEED analysis highlighted the significant importance of integrating RESs into electrical power systems. The findings clearly indicate that RESs integration plays a crucial role in reducing generation costs as well as lowering emission levels.

7. Conclusion

This study employed the MPA to identify the most efficient optimization technique for solving the DEED problem in electrical power systems. This was achieved through a comprehensive statistical comparison with other optimization methods, such as APO and PSO, to evaluate and validate the superiority of the proposed approach in terms of solution quality, stability, and computational performance. Furthermore, the effectiveness of the proposed method was tested on power systems of different scales to ensure the robustness and consistency of the obtained results. Subsequently, the ED of both systems was investigated over a 24-hour scheduling horizon, considering scenarios with and without RES integration, with the aim of minimizing both total operating cost and emission levels.

The results demonstrated the efficiency of MPA and its ability to achieve the lowest operating cost with high stability for both studied systems. In addition, the DEED analysis highlighted the significant importance of integrating RES into electrical power systems. The findings clearly indicate that RES integration plays a crucial role in reducing generation costs as well as lowering emission levels. Therefore, the study strongly recommends the adoption of renewable energy sources within the system framework due to their proven economic and environmental benefits.

Author Contributions: Authors have contributed significantly to the development and completion of this article.

Funding: This article received no external funding.

Acknowledgments: The authors thank the Ministry of Electricity, Water & Renewable Energies, Kuwait for providing laboratory facilities and equipment.

Ethics approval: The study used public system-level data and involved no human participants.

Conflicts of Interest: The author(s) declare no conflict of interest.

References

[1] A. Ezzat, A. A. Mahmoud, and A. A. A. Hafez, "Comprehensive review of artificial intelligence for shaping renewable energy power systems," *Solar Energy and Sustainable Development*, vol. 14, no. 1, pp. 504–521, Jul. 2025.

[2] A. Alazemi, H. Mohamed, A. Yossief, and A. Hafez, "Economic dispatch for hybrid power system," *Afro-Asian Journal of Scientific Research*, vol. 4, no. 1, pp. 409–421, 2026.

[3] M. Fakher, H. El-Khozondar, M. Mohammed, *et al*., "Assessing renewable energy penetration in the Libyan power sector," *Discover Sustainability*, 2026, doi: 10.1007/s43621-026-04483-0.

[4] I. Latiwash, M. Mohammed, M. A. Al Bari, *et al*., "Integrated energy economic environmental and technical assessment of an off-grid solar photovoltaic hydrogen system for electricity supply in Wadi Al Shati, Libya," *Discover Energy*, 2026, doi: 10.1007/s43937-026-00174-z.

[5] W. Salah *et al*., "Grid reliability enhancement via PV-diesel hybrid system in Palestine: Load flow analysis and CO_2 assessment," *Wadi Alshatti University Journal of Pure and Applied Sciences*, vol. 4, no. 1, pp. 436–452, 2026.

[6] M. Mohammed *et al*., "Renewable energy in Libya: A systematic review of resources, costs, and implementability," *Energy 360*, vol. 5, Art. no. 100066, 2026.

[7] A. Abduallah *et al*., "Leveraging hydrogen for covering energy shortage in an electricity subgrid," *Wadi Alshatti University Journal of Pure and Applied Sciences*, vol. 4, no. 1, pp. 245–254, 2026.

[8] A. Aisa, S. Alharari, E. Elarb, Y. Nassar, and H. El-Khozondar, "Design and analysis of an off-grid PV/wind/battery/diesel generator hybrid renewable power system for a healthcare facility in Gharyan, Libya," *Wadi Alshatti University Journal of Pure and Applied Sciences*, vol. 4, no. 2, pp. 68–91, 2026.

[9] M. Mohamed, A. Yousef, and A. Hafez, “Risk management strategies for fuel shortages in economic dispatch with multiple fuel options using walrus algorithm,” *Results in Engineering*, vol. 27, Art. no. 106427, 2025, doi: 10.1016/j.rineng.2025.106427.

[10] M. Mohamed, A. Yousef, and A. Hafez, “A novel metaheuristic optimizer GPSed via artificial intelligence for reliable economic dispatch,” *Scientific Reports*, vol. 15, no. 1, Art. no. 20258, 2025, doi: 10.1038/s41598-025-06648-9.

[11] D. Albuzia, A. Ali, M. Mohmed, and A. Hafez, “Reliable and robust optimal interleaved boost converter interfacing photovoltaic generator,” *Wadi Alshatti University Journal of Pure and Applied Sciences*, vol. 3, no. 2, pp. 192–201, 2025.

[12] M. Mohammed, E. Mohammed, R. Elzer, and Y. Nassar, “Techno-economic feasibility of parabolic trough solar steam for thermal enhanced oil recovery,” *Wadi Alshatti University Journal of Pure and Applied Sciences*, vol. 4, no. 1, pp. 184–190, 2026.

[13] M. Mohamed, A. Ali, A. Yousef, and A. Hafez, “Autonomous dynamic economic dispatch with limited fuel and renewable energy sources using marine predators optimizer,” *Scientific Reports*, vol. 16, no. 1, Art. no. 13518, 2026, doi: 10.1038/s41598-026-48247-2.

[14] M. Mohamed, A. Yousef, and A. Hafez, “Concise comparative study of economic dispatch of electrical power systems,” *Wadi Alshatti University Journal of Pure and Applied Sciences*, vol. 4, no. 1, 2026.

[15] M. Lotfi Akbarabadi and R. Sirjani, “Achieving sustainability and cost-effectiveness in power generation: Multi-objective dispatch of solar, wind, and hydro units,” *Sustainability*, vol. 15, no. 3, Art. no. 2407, 2023, doi: 10.3390/su15032407.

[16] H. Lotfi, “Presenting a novel hybrid method for dynamic economic/emission dispatch considering renewable energy units and energy storage systems,” *Evolutionary Intelligence*, vol. 18, no. 3, Art. no. 63, 2025, doi: 10.1007/s12065-025-01051-9.

[17] L. Li, Q. Shen, M.-L. Tseng, and S. Luo, “Power system hybrid dynamic economic emission dispatch with wind energy based on improved sailfish algorithm,” *Journal of Cleaner Production*, vol. 316, Art. no. 128318, 2021, doi: 10.1016/j.jclepro.2021.128318.

[18] M. Elnaggar, W. A. Salah, H. J. El-Khozondar, Y. F. Nassar, and M. J. K. Bashir, “Leveraging wind energy for electricity and hydrogen production: A sustainable solution to power shortages and eco-friendly alternative fuel,” *Advanced Energy and Sustainability Research*, vol. 7, no. 2, Art. no. e202500049, 2026, doi: 10.1002/aesr.202500049.

[19] M. Elnaggar, W. A. Salah, H. J. El-Khozondar, Y. F. Nassar, A. Ma’arif, M. J. K. Bashir, A. Abu Sneineh, M. Abuhelwa, B. Jarada, M. ALHabbash, and M. ALHabbash, “Harnessing solar energy for electricity generation and green hydrogen production: A sustainable pathway for low-carbon transportation in Gaza,” *International Journal of Energy Research*, vol. 2026, no. 1, Art. no. 8748862, 2026, doi: 10.1155/er/8748862.

[20] O. Shaltami, M. Ben Hkoma, K. Almahdi, F. Mohammed, M. Salem, and Y. Nassar, “Geochemical approaches to combating desertification and enhancing sustainable development in Libya,” *Wadi Alshatti University Journal of Pure and Applied Sciences*, vol. 4, no. 2, pp. 163–169, 2026.

[21] H. Rezk, A. Fathy, and M. A. Abdelkareem, “Optimal energy management of hybrid renewable power systems using advanced optimization techniques,” *Renewable Energy*, vol. 220, pp. 1197–1212, 2024.

[22] S. Kamel, M. Ebeed, and A. Ramadan, “Recent optimization techniques for economic dispatch in renewable-integrated power systems,” *IEEE Access*, vol. 12, pp. 21455–21478, 2024.

[23] Y. Zhang, X. Liu, and J. Wang, “Stochastic economic dispatch of power systems with wind and solar energy using metaheuristic optimization algorithms,” *Electric Power Systems Research*, vol. 228, Art. no. 110125, 2025.

[24] A. Faramarzi, M. Heidarinejad, S. Mirjalili, and A. H. Gandomi, “Marine predators algorithm: A nature-inspired metaheuristic,” *Expert Systems with Applications*, vol. 152, Art. no. 113377, 2020, doi: 10.1016/j.eswa.2020.113377.

[25] M. A. Elaziz, D. Yousri, and S. Mirjalili, “Marine predators optimizer for solving economic dispatch problems in power systems,” *Energy Reports*, vol. 7, pp. 5773–5789, 2021.

[26] S. Mirjalili and A. Lewis, “The whale optimization algorithm,” *Advances in Engineering Software*, vol. 95, pp. 51–67, 2016.
[27] M. Khaleel, Z. Yusupov, N. Yasser, and H. J. El-Khozondar, “Enhancing Microgrid Performance through Hybrid Energy Storage System Integration: ANFIS and GA Approaches”, ijees, vol. 1, no. 2, pp. 38–48, 2023, doi: 10.65998/ijees.v1i2.34.
[28] I. Imbayah *et al.*," Modeling a 600 MW floating photovoltaic system in Al-Khums City, Libya: Performance analysis and implementation using PVSyst," *Wadi Alshatti University Journal of Pure and Applied Sciences*, vol. 4, no. 1, pp. 223-237, 2026.
[29] A. A. Heidari and S. Mirjalili, “Recent advances in bio-inspired metaheuristic algorithms,” *Expert Systems with Applications*, vol. 198, Art. no. 116824, 2022.
[30] A. Fathy and H. Rezk, “Recent energy management strategies based on particle swarm optimization for hybrid renewable energy systems,” *Renewable Energy*, vol. 196, pp. 1071–1089, 2022.
[31] M. Pradhan, P. K. Roy, and T. Pal, “Oppositional-based grey wolf optimizer with PSO for economic dispatch problem,” *Journal of Electrical Systems and Information Technology*, vol. 9, no. 1, pp. 1–17, 2022.
[32] S. Kamel, A. Ramadan, and M. Ebeed, “Improved particle swarm optimization for solving optimal power flow and economic dispatch problems,” *IEEE Access*, vol. 11, pp. 31542–31555, 2023.
[33] M. I. Mohamed, A. M. Yousef, and A. A. Hafez, “Efficient and innovative dynamic power system economic dispatch for fuel shortages via walrus and artificial gorilla troops optimizers,” *Engineering Research Express*, vol. 7, no. 3, Art. no. 035303, 2025, doi: 10.1088/2631-8695/ade7f6.
[34] M. I. Mohamed, A. M. Yousef, and A. A. Hafez, “Optimized dynamic economic dispatch incorporating dynamic generation capacity using teaching-learning-based optimizer,” in *Proc. 15th International Conference on Electrical Engineering (ICEENG)*, Cairo, Egypt, 2025, pp. 1–6, doi: 10.1109/ICEENG64546.2025.11031333.
[35] M. Jin and M. Wang, “Research on the economic dispatch of power systems with a high proportion of renewable energy based on improved PSO,” *Journal of Physics: Conference Series*, vol. 2465, no. 1, Art. no. 012024, 2023, doi: 10.1088/1742-6596/2465/1/012024.
[36] A. Sabzevari, M. Moazzami, B. Fani, G. Shahgholian, and M. Hashemi, “Stochastic economic dispatch of a power system with solar farm considering generation flexibility and reliability,” *International Journal of Energy Research*, vol. 2024, no. 1, Art. no. 5528243, 2024, doi: 10.1155/2024/5528243.
[37] J. Soni and K. Bhattacharjee, “Multi-objective dynamic economic emission dispatch integration with renewable energy sources and plug-in electrical vehicle using equilibrium optimizer,” *Environment, Development and Sustainability*, vol. 26, no. 4, pp. 8555–8586, Apr. 2024, doi: 10.1007/s10668-023-03058-7.
[38] S. Acharya, S. Ganesan, D. V. Kumar, and S. Subramanian, “Optimization of cost and emission for dynamic load dispatch problem with hybrid renewable energy sources,” *Soft Computing*, vol. 27, no. 20, pp. 14969–15001, 2023, doi: 10.1007/s00500-023-08584-0.
[39] E. Salim *et al.*, “Performance evaluation of a standalone PV-hydrogen power system for continuous supply reliability in Brack Al-Shatti,” *Wadi Alshatti University Journal of Pure and Applied Sciences*, vol. 4, no. 1, pp. 362–376, 2026.
[40] H. El-Khozondar *et al.*, “Analysis of a grid/wind/hydrogen hybrid energy system for producing electricity, vehicle fuel and freshwater for Gaza Strip-Palestine,” *Fuel*, vol. 428, Art. no. 140358, 2027, doi: 10.1016/j.fuel.2026.140358.
[41] J. Qiu, D. Lan, Y. Zhang, and H. Li, “Multi-objective reactive power optimization for low-voltage distribution networks based on improved marine predator algorithm,” *Journal of Physics: Conference Series*, vol. 2703, no. 1, Art. no. 012050, 2024, doi: 10.1088/1742-6596/2703/1/012050.
[42] R. Özdemir, M. Taşyürek, and V. Aslantaş, “An improved marine predators algorithm for shipment status time estimation and regression problems,” *International Journal of Machine Learning and Cybernetics*, vol. 17, no. 2, Art. no. 66, 2026, doi: 10.1007/s13042-025-02967-5.
[43] S. Lee, M. H. Almomani, S. A. Alomari, and K. Saleem, “A novel deep learning framework with artificial protozoa optimization-based adaptive environmental response for wind power

prediction," *Scientific Reports*, vol. 15, no. 1, Art. no. 18746, 2025, doi: 10.1038/s41598-025-97793-8.

[44] X. Wang, V. Snášel, S. Mirjalili, J. Pan, L. Kong, and H. A. Shehadeh, "Artificial Protozoa Optimizer (APO): A novel bio-inspired metaheuristic algorithm for engineering optimization," *Knowledge-Based Systems*, vol. 295, Art. no. 111737, 2024, doi: 10.1016/j.knosys.2024.111737.

[45] M. Shehab, "Artificial protozoa optimizer: A bio-inspired metaheuristic for complex engineering optimization," *Results in Engineering*, vol. 27, Art. no. 106883, 2025, doi: 10.1016/j.rineng.2025.106883.